JACS
JOURNAL OF THE AMERICAN CHEMICAL SOCIETY

Article

pubs.acs.org/JACS

The Interaction of Fluoride with Fluorogenic Ureas: An ON^1–OFF–ON^2 Response

Valeria Amendola,*[,†] Greta Bergamaschi,[†] Massimo Boiocchi,[‡] Luigi Fabbrizzi,*[,†] and Lorenzo Mosca[§]

[†]Dipartimento di Chimica, Università di Pavia, via Taramelli 12, 27100 Pavia, Italy

[‡]Centro Grandi Strumenti, Università di Pavia, via Bassi 21, 27100 Pavia, Italy

[§]Department of Chemistry and Center for Photochemical Sciences, Bowling Green State University, Bowling Green, Ohio 43403-0001, United States

Supporting Information

ABSTRACT: The anion binding tendencies of the two fluorogenic ureas L^1H and L^2H, containing the 2-anthracenyl and 1-pyrenyl moieties as signaling units, respectively, have been investigated in MeCN and DMSO by absorption, emission, and ^1H NMR spectroscopies. The formation of stable 1:1 receptor:anion H-bond complexes has been confirmed by structural studies on the crystalline $[Bu_4N][L^1\cdots Cl]$ and $[Bu_4N][L^2H\cdots CH_3COO]$ salts. Complexation induces significant variations of the emission properties of L^1H and L^2H according to a multifaceted behavior, which depends upon the fluorogenic substituent, the solvent, and the basicity of the anion. Poorly basic anions (Cl^-, Br^-) cause a red shift of the emission band(s). Carboxylates (CH_3COO^-, $C_6H_5COO^-$) induce fluorescence quenching due to the occurrence of an electron-transfer process taking place in the locally excited complex $[*L\text{-}H\cdots X]^-$. However, this excited complex may undergo an intracomplex proton transfer from one urea N–H fragment to the anion, to give the tautomeric excited complex $[L\cdots H\text{–}X]^{-*}$, which emits at higher wavelength. F^- displays a unique behavior: It forms with L^1H a stable $[L\text{–}H\cdots F]^-$ complex which in the excited state undergoes intracomplex proton transfer, to give the poorly emissive excited tautomer $[L\cdots H\text{–}F]^{-*}$. With L^2H, on moderate addition of F^-, the 1:1 H-bond complex forms, and the blue fluorescence of pyrene is quenched. Large excess addition of F^- promotes deprotonation of the ground-state complex, according to the equilibrium $[L^2H\cdots F]^- + F^- \leftrightarrows [L^2]^- + HF_2^-$. The deprotonated receptor $[L^2]^-$ is distinctly emissive (yellow fluorescence), which generates the fluorimetric response ON^1–OFF–ON^2 of receptor L^2H with respect to F^-.

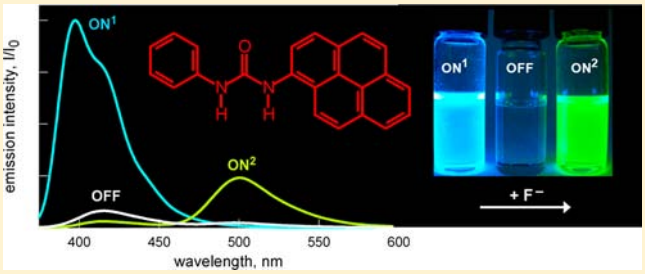

INTRODUCTION

Design and synthesis of chromogenic and fluorogenic sensors for anions are lively and quickly developing subdisciplines of supramolecular chemistry.[1,2] Most sensors belonging to this class of urea derivatives are neutral and contain a subunit capable of donating H-bonds to the anion.[3] A great number of optical anion sensors of varying complexity, containing one or more urea moieties, have been synthesized over the last two decades.[4,5] The design usually involves the covalent linking of an optically responsive fragment to an urea subunit. Anion recognition occurs through the H-bonding interaction of urea N–H protons with the anion, to give a stable anion–receptor complex. In the case of chromogenic sensors, complex formation is instrumentally signaled by a red shift of charge-transfer absorption band(s) and visually by a neat color change. In particular, the negative charge brought by the anion stabilizes the excited state of the chromophore, thus reducing the energy of the urea-to-chromophore charge-transfer transition.

Among investigated anions, a special attention has been devoted to fluoride. This is certainly due to the prominent role played by F^- in biology, medicine, food, and environmental sciences.[6] Besides, fluoride shows a versatile and distinctive behavior when interacting with N–H containing receptors, including urea: As the anion of the most electronegative element and as a fairly strong Brønsted base, it forms H-bond complexes, whose stability is rivaled only by acetate and other carboxylates. Moreover, addition of excess fluoride may promote the deprotonation of one N–H fragment of the urea subunit, a process favored by the presence of strongly electron-withdrawing groups on the receptor (e.g., 4-nitrophenyl) and driven by the unique stability of the HF_2^- complex.[7] Deprotonation of one N–H fragment is accompanied by a drastic electron rearrangement on the receptor, which results in a significant change of both the absorption spectrum and the color as well as of the pattern of ^1H NMR signals, which makes the process unambiguously discernible.[8] A number of urea based optical sensors of fluoride have been reported in the past decade, in which different chromogenic and fluorogenic substituents had been covalently linked to the binding subunit.[9]

Received: March 1, 2013
Published: April 1, 2013

   dx.doi.org/10.1021/ja4019786 | J. Am. Chem. Soc. 2013, 135, 6345–6355

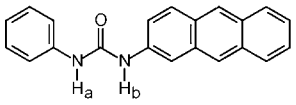

L^1H

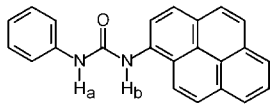

L^2H

Recently, Arai et al. investigated the interaction of the 2-anthracenyl-urea receptor L^1H with acetate in DMSO and demonstrated that a neat proton transfer from urea to CH_3COO^- takes place in the excited state.[10] In particular, on formation of the $[L^1H\cdots CH_3COO]^-$ complex, the emission of the anthracenyl fluorophore was quenched, while a new emission band developed at lower energies. It was suggested, on the basis of time-dependent fluorescence decay and time-resolved spectra, that such a band originates from a charge-transfer transition involving a tautomeric form of the complex, in which a proton had been transferred from urea to X^-.

In this study, we report on the behavior of the new fluorescent anion receptor L^2H, containing a 1-pyrenyl substituent, whose binding properties toward a variety of anions (halides, carboxylates) are compared to those of the 2-anthracenyl analogue L^1H, under the same conditions. Both receptors contain a fluorescent unit integrated with the urea binding site. In this situation, absorption and emission properties of the receptors are sensitive to the H-bond acceptor behavior and to the basicity of the interacting anion. On anion interaction at the urea subunit, negative charge is transferred onto the urea substituents. It is expected that this negative charge can be delocalized onto the pyrenyl moiety to a larger extent than onto the anthracenyl subunit, a circumstance which may affect the receptor's response. These aspects have been investigated in detail by absorption, emission, and ^1H NMR spectroscopies. X-ray diffraction studies on the crystalline $[Bu_4N][L^1H\cdots Cl]$ and $[Bu_4N][L^2H\cdots CH_3COO]$ salts have helped to define the nature of the receptor–anion interaction in the ground state. It is anticipated that the response of L^2H to F^- is unique, as, on addition of a moderate excess of anion, the emission band at 400 nm (blue fluorescence, output 1) is quenched, while, on addition of a large excess of F^-, a new emission band develops at 500 nm (yellow fluorescence, output 2), thus giving rise to an ON^1–OFF–ON^2 fluorescent response to fluoride. Such a behavior is essentially related to proton-transfer processes from one urea N–H fragment in the excited-state H-bond complex, to the H-bonded F^- (first step), and in the ground-state complex, to give the deprotonated receptor and HF_2^- (second step). An ON^1–OFF–ON^2 response to F^- had been previously reported for receptors containing covalently linked naphthol and imidazole subunits.[11] Such a behavior originated from the fact that the proton transfer from the naphtholic O–H fragment to the facing imidazole nitrogen atom, typically taking place in the excited state of the uncomplexed receptor, was inhibited by fluoride complexation.

EXPERIMENTAL PROCEDURES

General. All reagents were purchased by Aldrich. Tetrabutylammonium salts were all >98% pure and dried *in vacuo* overnight before use. The solutions used in titrations were prepared from freshly opened solvent bottles. Mass spectra were acquired on a Thermo-Finnigan ion-trap LCQ Advantage Max instrument equipped with an ESI source. NMR spectra were taken on a Bruker AVANCE 400 spectrometer (operating at 9.37 T, 400 MHz). UV–vis spectra were run on a Varian Cary 100 SCAN spectrophotometer with quartz cuvettes of the appropriate path length (0.1–1 cm) at 25.0 ± 0.1 °C under inert conditions. Emission spectra were recorded on a Perkin-Elmer LS 50B instrument. Fluorescence spectra at 77 K were measured using quartz sample tubes and a low-temperature luminescence accessory (Perkin-Elmer). Synthesis and characterization of receptors L^1H and L^2H are described in the Supporting Information.

Spectrophotometric and Spectrofluorimetric Titrations. Titrations were performed at 25.0 ± 0.1 °C in MeCN and DMSO. In a typical experiment, the solution of the receptor (L^1H, L^2H) was titrated with a 100-fold more concentrated solution of the tetrabutylammonium salt of the envisaged anion. In spectrofluorimetric titrations, the sample was excited at a wavelength corresponding to an isosbestic point in the UV–vis spectra. Titration data were processed with a nonlinear least-squares procedure (Hyperquad package),[12] in order to determine the equilibrium constants. Fluorescent spectra at 77K were measured in butyronitrile.

^1H NMR Spectroscopy Titrations. All experiments were performed at 25.0 ± 0.1 °C in d^6-DMSO. Equilibrium constants were determined by processing data with Hyperquad.[12]

X-ray Crystallographic Studies. Diffraction data were collected at ambient temperature by means of a Bruker-Axs CCD-based diffractometer working with graphite-monochromatized $Mo_{K\alpha}$ X-radiation (λ = 0.71073 Å). Crystal data are reported in Table S4. All the investigated compounds were constituted by platy laminar single crystals, whose thickness was <20 μm. Selected crystals of L^1H and of its $[L^1H\cdots Cl]^-$ complex (occurring as a tetrabutylammonium, partly hydrated salt) showed diffraction quality suitable to collect good diffraction data until a θ_{max} value of 25°. On the contrary, the single crystal of the $[L^2H\cdots CH_3COO]^-$ complex (occurring as a tetrabutylammonium salt) exhibited poor X-ray diffraction quality, and diffracted intensities with θ values >23.5° were unobservable.

Frames collected by the CCD-based system were processed with the SAINT software,[13] and intensities were corrected for Lorentz and polarization effects. Absorption effects were empirically evaluated by the SADABS software,[14] and absorption correction was applied to the data. Crystal structures were solved by direct methods (SIR 97)[15] and refined by full-matrix least-squares procedures on F^2 using all reflections (SHELXL 97).[16] Anisotropic displacement parameters were refined for all nonhydrogen atoms. Hydrogens bonded to carbon atoms were placed at calculated positions with the appropriate AFIX instructions and refined using a riding model. Hydrogens bonded to N atoms were located in the final ΔF maps; their positions were refined during the final least-squares procedures restraining the N–H distance to the value 0.96 ± 0.01 Å. In the crystal of the chloride complex, a fourth part of the O1w site is populated by oxygen of a partly present water solvent molecule.

RESULTS AND DISCUSSION

Anion Interactions with Receptor L^1H in the Ground State: Spectrophotometric and ^1H NMR Studies. The binding tendencies of L^1H in its ground state have been first investigated through spectrophotometric titrations with the tetrabutylammonium salts of halides and carboxylates, in MeCN and DMSO. The family of spectra taken over the course of the titration of an MeCN solution of L^1H with $[Bu_4N]F$ is shown in Figure 1, while spectra from titration with $[Bu_4N]Cl$ are shown in Figure S1. The absorption spectrum of the free receptor L^1H shows intense bands with a well-defined vibrational structure over the 320–380 nm interval, in both MeCN and DMSO. In MeCN, the maxima are blue-shifted of ~5 nm with respect to DMSO. Upon fluoride addition, the absorption bands of receptor L^1H undergo a significant red shift, which reflects the stabilization of the excited state following the interaction with the anion.

Best fitting of titration data through a nonlinear least-squares procedure (using the program HyperQuad)[12] was obtained on assuming the occurrence of the equilibrium: $L^1H + F^- \leftrightarrows [L^1H\cdots F]^-$. Figure 1, inset, shows that absorbance at 308 nm

dx.doi.org/10.1021/ja4019786 | J. Am. Chem. Soc. 2013, 135, 6345–6355

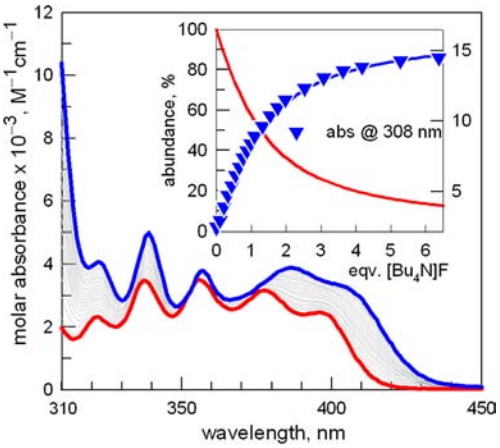

Figure 1. UV−vis spectra taken over the course of titration of receptor L^1H (0.07 mM) with $[Bu_4N]F$ in MeCN. Inset: lines are concentration profiles of the species at the equilibrium L^1H (red line) and $[L^1H\cdots F]^-$ (blue line), left vertical axis; and symbols are molar absorbance at 308 nm, right vertical axis.

superimposes well on the concentration profile of the $[L^1H\cdots F]^-$ complex. Log K values associated to the complexation equilibria involving halide and carboxylate ions are reported in Table 1.

Table 1. Association Constants (as log K values) for the Equilibrium: $LH + X^- \leftrightarrows [LH\cdots X]^-$ ($LH = L^1H, L^2H$), Studied in Pure Organic Solvents (i.e. MeCN and DMSO) at 25°C[a]

L^1H	Cl^-	Br^-	CH_3COO^-	$PhCOO^-$	F^-
MeCN	3.46(1)[b]	2.66(1)[b]	5.35(1)[b]	5.04(1)[b]	4.27(1)[b]
	3.56(1)[c]	3.05(1)[c]	5.41(1)[c]	5.05(1)[c]	4.23(1)[c]
DMSO	na	na	3.47(1)[b]	3.0(1)[b]	2.9(1)[b]
L^2H	Cl^-	Br^-	CH_3COO^-	$PhCOO^-$	F^-
MeCN	3.58(1)[b]	2.71(1)[b]	5.02(1)[b]	4.24(1)[b]	4.45(1)[b]
	3.71(1)[c]	2.86(1)[c]	5.04(1)[c]	4.18(1)[c]	4.52(1)[c]

[a]Standard deviation on the last figure; and na = not available. [b]K values were determined via UV−vis spectroscopy. [c]K values were determined via emission spectroscopy.

Anion affinity is lower in DMSO than in MeCN, due to the more pronounced competing effect of DMSO as an H-bond acceptor. In MeCN, anion affinity for L^1H decreases along the series $F^- > Cl^- > Br^-$, which reflects the decreasing tendency of the anion to receive H-bonds. Most stable complexes are given by the carboxylates, a behavior probably related to the capability of these anions to establish with urea two parallel O···H−N H-bonds. No N−H deprotonation was observed even after a large excess addition of fluoride in both investigated media, which reflects the relatively poor electron-withdrawing tendencies of the aromatic substituents (i.e., 2-anthracenyl and phenyl).

Results of ^1H NMR titrations were consistent with those obtained from UV−vis titration experiments. As a representative example, Figure 2 displays the family of spectra recorded over the course of the ^1H NMR titration of L^1H with $[Bu_4N]CH_3COO$ in d^6-DMSO. Both N−H signals are shifted downfield upon acetate addition, the strong deshielding of the corresponding resonances ($\Delta\delta$ = 3.3 ppm for both N−Hs) being consistent with the strong polarization induced by the H-bonded carboxylate anion. The association constant obtained from the curve fitting of ^1H NMR titration profiles, log K_{NMR} = 3.5(1), is very close to that determined under similar conditions by Arai [10] and to that determined in this work by UV−vis titration in DMSO (see Table 1).

X-ray Crystal Structures of L^1H and $[Bu_4N][L^1H\cdots Cl]$. Both the uncomplexed receptor L^1H and its 1:1 chloride complex were isolated as crystalline materials. Suitable crystals for X-ray crystallographic analysis were obtained by slow diffusion of diethyl ether on MeCN solutions. The molecular structures of L^1H and $[L^1H\cdots Cl]^-$ are reported in Figure 3. In both uncomplexed and complexed receptor, the two aromatic arms are bent with respect to the conjugated central urea subunit (see Supporting Information for details) and are nearly orthogonal to each other, with a torsion angle of 83.9(1)°. The structure gives rise to extended intermolecular H-bonding networks, which are quite common in similar diaryl-urea derivatives.[5] The bifurcated H-bonded urea tape, described in detail in the Supporting Information (see Figure S2 and Table S1), is probably responsible for the low solubility of L^1H in MeCN ($<10^{-4}$ M at 25 °C). However, the urea subunit maintains some degree of freedom, as evidenced by the nonparallel arrangement of the two N−H bonds. In particular, one of the two H-atoms lies in the best plane of the urea group, whereas the other one is displaced from the best plane by 0.25(4) Å. The relative position of the urea's H-atoms observed in the crystalline structure of the free receptor L^1H does not seem favorable to the establishment of H-bonds. However, the interaction with anions induces a drastic conformational change in the receptor' structure, strongly increasing its planarity (see Figure S3 and Table S2). In particular, in the chloride complex $[L^1H\cdots Cl]$ (see Figure 3b), the N−H bonds of the urea subunit are parallel. Moreover, the two protons lie out of the best plane of urea only by 0.17(5) Å and interact with chloride forming a six-membered ring.

The aromatic substituents are now almost coplanar, with a dihedral angle between the two best planes of 13.9(2)°. The small deviation from planarity can be ascribed to crystal packing effects associated with the asymmetrical position of the tetrabutylammonium ion. The interaction with the anion also disrupts the intermolecular urea tape made by receptor molecules, which may explain the increased solubility in MeCN.

Fluorimetric Response of L^1H to Anions. At room temperature, the emission spectrum of L^1H is characterized by a nonstructured broad band, centered at 439 nm (λ_{exc} = 366 nm) in MeCN and 446 nm (λ_{exc} = 352 nm) in DMSO. The emissive species corresponds to the locally excited (LE) state $^*L^1H$.[10] On anion addition, a different behavior was observed depending upon solvent polarity and anion basicity.

In the less polar solvent MeCN, addition of poorly basic anions (Cl^- and Br^-) to a solution of L^1H induces a red shift of the emission band. Figure 4a shows the family of spectra obtained over the course of the titration of a solution 0.01 mM of L^1H with $[Bu_4N]Cl$. Titration profiles were satisfactorily fitted for the equilibrium $L^1H + X^- \leftrightarrows [L^1H\cdots X]^-$ ($X^- = Cl^-$, Br^-), whose association constant showed values consistent with those determined through spectrophotometric titrations (see Table 1). The red shift induced by complexation (from 439 to 445 nm in the case Cl^-) reflects the stabilization of the excited state following H-bond interaction with the anion (route (b) in Figure 5).

dx.doi.org/10.1021/ja4019786 | J. Am. Chem. Soc. 2013, 135, 6345−6355

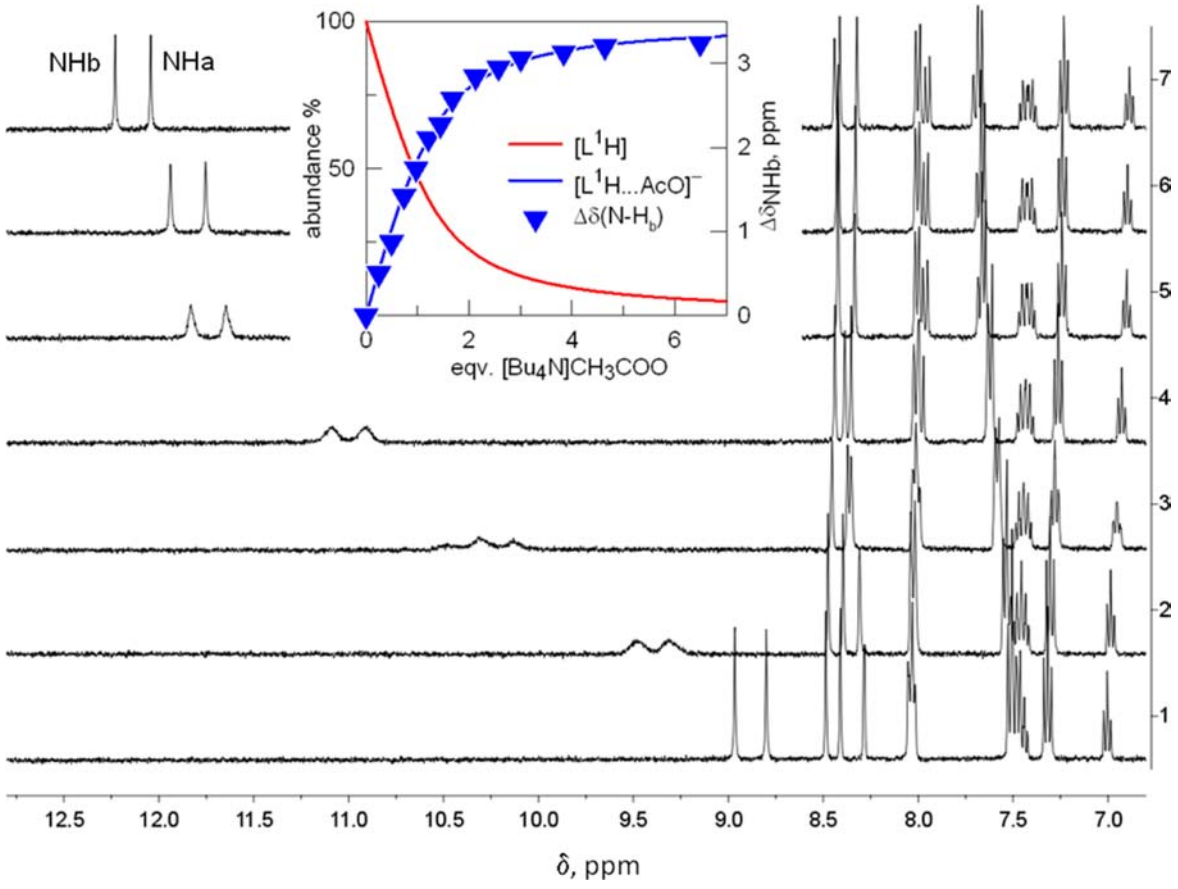

Figure 2. ^{1}H NMR spectra taken over the course of titration of receptor L^{1}H (1.2 mM) with $[Bu_4N]CH_3COO$ in d^6-DMSO. Spectrum 1: uncomplexed receptor. Spectra 2−7: after the addition of 0.3, 0.5, 0.7, 1.0, 1.5, 3.0 equiv of $[Bu_4N]CH_3COO$. Inset: lines are concentration profiles of $[L^1H]$ and $[L^1H\cdots CH_3COO]^-$, and symbols are variation of the chemical shift of the N−H$_b$ proton.

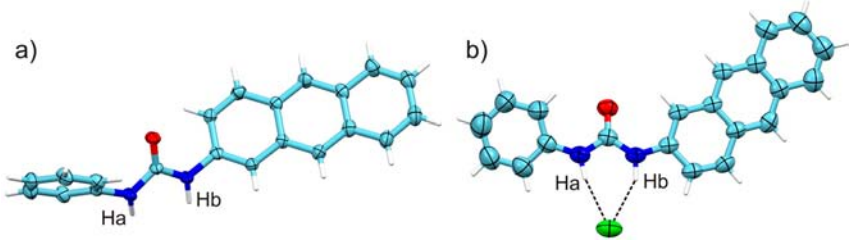

Figure 3. Molecular structures of (a) L^{1}H and (b) $[L^1H\cdots Cl]^-$; the tetrabutylammonium ion has been omitted for clarity. For more detailed ORTEP views see Figures S2 and S3 (significant bond distances and angles in Tables S1 and S2).

On the other hand, titration of L^{1}H with more basic anions (F^-, CH_3COO^-, $C_6H_5COO^-$) induced a substantial quenching of the anthracene emission band. Moreover, the residual emission band appeared red-shifted, to a similar extent as observed for Cl^-. Figure 4b shows, as an example, the family of spectra taken over the course of the titration of L^{1}H with $[Bu_4N]CH_3COO$. It is suggested that quenching is due to an electron-transfer (eT) process from the carbonyl oxygen atom of the urea subunit, which, on interaction with the anion, has assumed a partial negative charge, to the facing excited anthracenyl moiety. In particular, electron density has been transferred to the oxygen atom from the coordinated anion through H-bonds.

The eT nature of the quenching process was demonstrated by taking spectra at low temperature. In fact, the eT process and the associated separation of electrical charges involve the reorganization of the solvent molecules bound to receptor. Freezing at the liquid nitrogen temperature immobilizes solvent molecules, thus preventing their reorganization and ultimately the occurrence of the eT process, which makes fluorescence revive. Indeed, a vitrified solution of L^{1}H containing an excess of CH_3COO^-, in butyronitrile at 77K, displayed an intense and well-defined emission band (see Figure S4), thus confirming the occurrence of an intracomplex eT process in the liquid solution at room temperature.

The mechanism of the anthracene quenching through an eT process within the $[^*L-H\cdots X]^-$ locally excited complex (L−H = L^{1}H) is illustrated in Figure 5, route (a). Fluoride and benzoate ions showed the same behavior as acetate.

The interaction of L^{1}H with basic anions (F^- and carboxylates) in DMSO produced a distinctly different response. Figure 6a shows, as an example, the family of spectra

dx.doi.org/10.1021/ja4019786 | J. Am. Chem. Soc. 2013, 135, 6345−6355

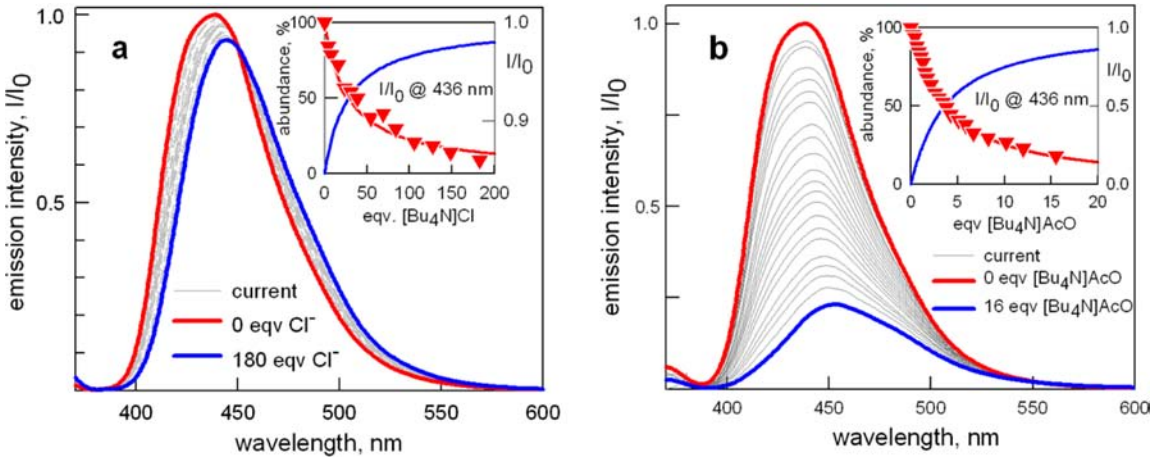

Figure 4. Emission spectra taken over the course of titration of receptor L^1H (0.01 mM) in MeCN with (a) $[Bu_4N]Cl$ and (b) $[Bu_4N]CH_3COO$. Insets: lines are concentration profiles of the species at the equilibrium, L^1H (red) and $[L^1H\cdots X]^-$ (blue), left vertical axis; and symbols are values of I/I_0 at 436 nm, right vertical axis. The excitation wavelength, λ_{exc} = 366 nm, corresponds to an isosbestic point observed in the UV−vis titration.

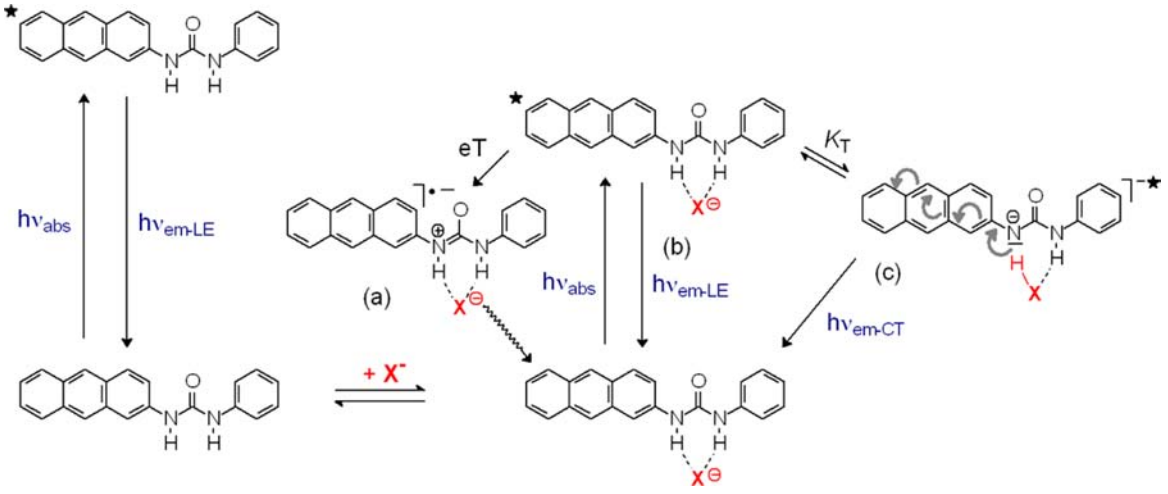

Figure 5. A qualitative sketch of the emissive behavior of the $[L^1H\cdots X]^-$ complex. Route (a): $X^- = CH_3COO^-$, F^- in MeCN, quenching of the locally excited (LE) complex $[^*L^1H\cdots X]^-$ by eT from the partially negatively charged carbonyl oxygen atom. Route (b) $X^- = Cl^-$, Br^-: emission of the LE complex $[^*L^1H\cdots X]^-$ (red-shifted with respect to the uncomplexed receptor $^*L^1H$. Route (c): $X^- = F^-$, CH_3COO^- in DMSO. Charge transfer (CT) emission of the excited tautomeric complex originated from the proton transfer from one N−H fragment to X^-; π-delocalization over the anthracenyl subunit is purely indicative.

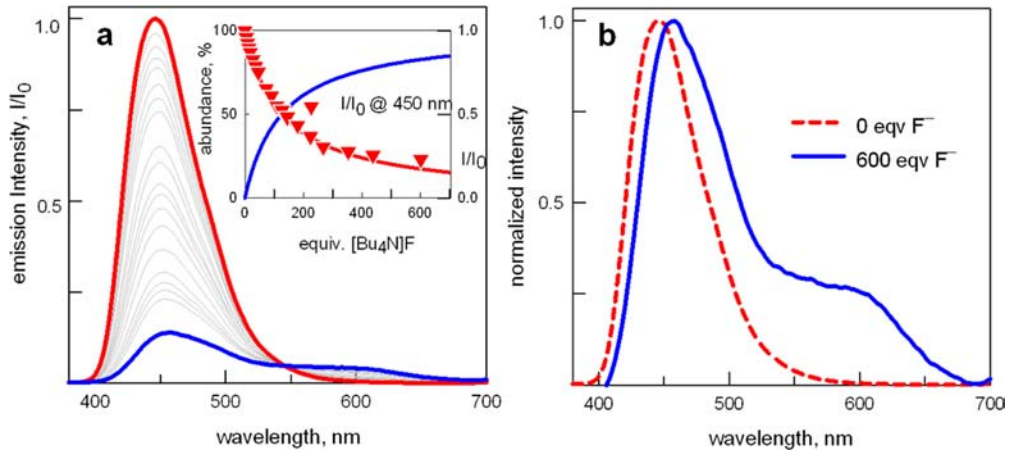

Figure 6. (a) Emission spectra taken over the course of titration of receptor L^1H (0.01 mM) with $[Bu_4N]F$ in DMSO (λ_{exc} = 352 nm). Inset: lines are concentration profiles of the species at the equilibrium: L^1H (red line) and $[L^1H\cdots F]^-$ (blue line); and symbols are relative emission intensity at 450 nm. (b) Normalized emission spectra of receptor L^1H (0.01 mM) both in the absence and in the presence of excess $[Bu_4N]F$.

dx.doi.org/10.1021/ja4019786 | J. Am. Chem. Soc. 2013, 135, 6345−6355

taken over the course of the titration of L^1H with $[Bu_4N]F$. Anion addition quenches the emission band centered at 450 nm, as observed for the titration in MeCN. However, quenching of the band at 450 nm is accompanied by the simultaneous development of a less intense, still detectable band centered at 600 nm. The formation of such an emission band is fully evident in the normalized spectrum in Figure 6b. Such a behavior has been previously observed in the titration of L^1H with acetate in DMSO[10] and has to be ascribed to the charge-transfer emission of a tautomer form of the locally excited complex $[*L{-}H{\cdots}X]^-$. This species originates from an intracomplex proton transfer from one urea's N−H fragment to X^- and is properly described by the formula $[L{\cdots}H{-}X]^{-}*$. The process is illustrated by route (c) in Figure 5. The interconnection of the two excited states is demonstrated by the fact that excitation spectra corresponding to λ_{em} = 455 and 600 nm are the same.

It remains now to explain why the excited-state tautomer $[L{\cdots}H{-}X]^{-}*$ forms in DMSO and not in MeCN. In this connection, it is useful to consider the H-bonding interaction as a frozen proton-transfer process from the H-bond donor (e.g., urea's N−H fragment) to the acceptor (the anion X^-, in the present case).[17] Such a process is controlled by anion basicity: The more basic the anion, the more advanced the proton transfer. Also the solvent controls the advancement of the proton transfer. In particular, a polar solvent is expected to stabilize the deprotonated receptor, thus favoring the occurrence of a complete proton transfer from N−H to X^-. N−H deprotonation of urea based receptors in their ground state requires the presence of powerful electron-withdrawing substituents directly linked to the urea subunit (e.g., nitrophenyl) and occurs only in the presence of excess fluoride, with formation of the highly stable HF_2^- self-complex.[8] It is now demonstrated that photoinduced proton transfer takes place also with moderately acidic urea subunits and does not involve formation and release of any HX_2^- species.

Anion Interactions with Receptor L^2H in the Ground State: Spectrophotometric and ^1H NMR Studies. The affinity of receptor L^2H toward anions was investigated by UV−vis and ^1H NMR spectroscopies. In both MeCN and DMSO, the absorption spectrum of receptor L^2H shows a well-defined vibrational pattern over the 300−400 nm interval, which is similar, for instance, to that observed with 1-aminopyrene derivatives.[18] In titration experiments in MeCN, a well-defined red shift of the absorption bands of receptor L^2H was observed following addition of any investigated anion. Figure 7 shows the family of UV−vis spectra taken upon titration of L^2H with $[Bu_4N]CH_3COO$ in MeCN, in which a 15-fold excess of anion was added (for the UV−vis titration with $[Bu_4N]Cl$ see Figure S5).

Best fitting of spectrophotometric titration data was in any case obtained by assuming the occurrence of the equilibrium: $L^2H + X^- \leftrightarrows [L^2H{\cdots}X]^-$. Corresponding association constants are reported in Table 1. The affinity trend and log K values are quite similar to those observed for receptor L^1H, which reflects a comparable effect of polyaromatic substituents, whether anthracenyl or pyrenyl, on the acidity of the urea N−H fragments in the two receptors.

In DMSO, the absorption maxima of the free receptor are red-shifted by ∼11 nm with respect to MeCN. Such a significant shift may be attributed to the relatively intense H-bond interaction of DMSO with the urea unit. This perturbation is very similar to that induced by anions. Thus,

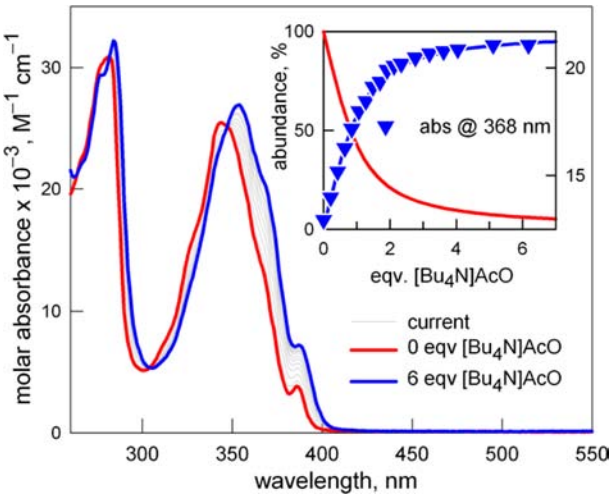

Figure 7. UV−vis spectra taken over the course of titration of receptor L^2H (0.03 mM) with $[Bu_4N]CH_3COO$ in MeCN. Inset: lines are concentration profiles of the species at the equilibrium: L_2H (red) and $[L_2H{\cdots}CH_3COO]^-$ (blue), left vertical axis; and symbols are molar absorbance at 368 nm, right vertical axis.

replacing of DMSO molecules by any added anion does not induce any significant modification of the UV−vis spectrum and prevents from carrying out spectrophotometric titrations in DMSO.

However, anion binding in DMSO could be successfully investigated by ^1H NMR titration experiments. The family of ^1H NMR spectra taken on titration of L^2H with $[Bu_4N]CH_3COO$ in d^6-DMSO is reported in Figure S6. Upon acetate addition, both N−H protons shift downfield. However, the N−H fragment close to the pyrenyl fragment (N−H_b in Figure S6) is more affected by acetate coordination, as indicated by the larger shift ($\Delta\delta_{N-H_b}$ = +2.84 ppm; $\Delta\delta_{N-H_a}$ = +2.35 ppm). From the nonlinear least-squares fitting of the titration profile (δ_{N-H_b} vs equiv $[Bu_4N]CH_3COO$, see Figure S7), an association constant log K_{NMR} = 3.1(1) could be determined. Also the pyrenyl C−H protons adjacent to the urea fragment are affected by anion binding. In particular, C−H_β and C−H_α significantly shift up- and downfield, respectively ($\Delta\delta_{CH_\beta}$ = −0.23 ppm; $\Delta\delta_{CH\alpha}$ = +0.21 ppm). These effects—more pronounced downfield shift of N−H_b and significant shifts of C−H_β and C−H_α—may be related to the geometrical properties of the complex and to the coordination mode of acetate, as indicated by structural features revealed by studies on the crystalline complex $[Bu_4N][L^2H{\cdots}CH_3COO]$ (*vide infra*).

X-ray Crystal Structure of $[Bu_4N][L^2H{\cdots}CH_3COO]$. Suitable crystals for X-ray crystallographic analysis were obtained by slow diffusion of diethyl ether to an equimolar solution of L^2H and $[Bu_4N]CH_3COO$ in MeCN. The cell unit contains two nonsymmetrically equivalent forms of the complex salt $[Bu_4N][L^2H{\cdots}CH_3COO]$. Only one of the two forms is reported in Figure 8 (the whole structure in shown in Figure S8 and Table S3).

Quite interestingly, each urea unit of the two independent receptors forms two bifurcate H-bonds with one oxygen atom of each acetate anion (mean $d_{NH_a\cdots O}$ = 1.80(8) Å; mean $d_{NH_b\cdots O}$ = 1.92(9) Å). Usually, urea donates two parallel H-bonds to two oxygen atoms of carboxylate ions. The bifurcate binding

dx.doi.org/10.1021/ja4019786 | J. Am. Chem. Soc. 2013, 135, 6345−6355

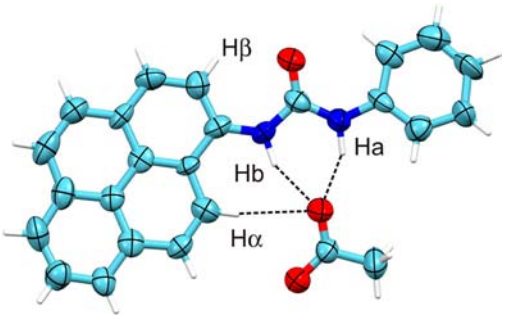

Figure 8. Molecular structure of one of the two nonequivalent forms of the complex $[L^2H\cdots CH_3COO]^-$ (the $[Bu_4N]^+$ ion has been omitted for clarity). More details are given in Figure S8.

mode observed here is quite uncommon, except for receptors containing two or more urea moieties.[19] In the $[L^2H\cdots CH_3COO]^-$ complex, the stabilization of the bifurcate mode is probably due to the presence of a C−H···O interaction between the carboxyl oxygen and C−H_α of the pyrene ring (mean $d_{CH_\alpha\cdots O}$ = 2.45(1) Å). It is possible that such an arragement is a consequence of steric effects. However, the bifurcate mode of interaction is consistent with the deshielding of the C−H_α proton, observed in d^6-DMSO solution. In the crystal structure of $[L^2H\cdots CH_3COO]^-$, the receptor remains almost coplanar. In particular, the dihedral angles between the phenyl arm and the pyrenyl subunit in the two independent receptor moieties are 12.8(5) and 17.3(5)°, respectively. Again, the deviation from planarity at the solid state can be ascribed to the steric requirements imposed by the $[Bu_4N]^+$ cations to the crystal packing.

Fluorimetric Response of L^2H to Anions. Upon excitation at 348 nm, the emission spectrum of L^2H in MeCN shows maxima at 394 and 412 nm. On titration of L^2H with Cl^- and Br^-, a red shift of the emission bands was observed. Figure 9 shows the emission spectra obtained for Cl^- (λ_{exc} = 348 nm, i.e., the isosbestic point observed in the UV−vis titration). Best fitting of the titration profiles was obtained on

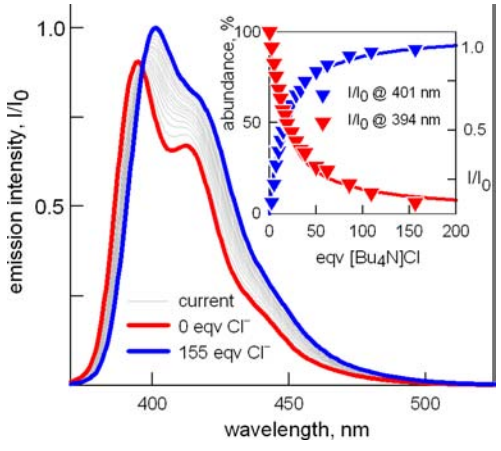

Figure 9. Emission spectra taken upon titration of L^2H (0.01 mM) in MeCN with $[Bu_4N]Cl$. The excitation wavelength, λ_{exc} = 348 nm, corresponds to an isosbestic point observed in the UV−vis titration. Inset: lines are concentration profiles of the species at the equilibrium: L^2H (red line) and $[L^2H\cdots Cl]^-$ (blue line), left vertical axis; and symbols are relative emission intensities at selected wavelengths, right vertical axis. T = 25 °C.

assuming the formation of 1:1 receptor−anion complexes, whose association constants are reported in Table 1 and satisfactorily compared to those obtained from UV−vis titrations. In DMSO, no variation of the pyrene emission was detected on addition of either Cl^- or Br^-, presumably because solvent and anions exert a similar perturbing effect on the excited state, in analogy to what was observed in absorbance measurements. On the other hand, in both MeCN and DMSO, the more basic carboxylate anions induced a substantial quenching of the pyrene emission. This circumstance allowed the determination of association constants from fitting of titration data. Corresponding values, reported in Table 1, are in good agreement with those determined through UV−vis titration experiments.

Acetate displays a distinctly different behavior. Figure 10a shows the family of emission spectra obtained on titration of L^2H (0.01 mM) with $[Bu_4N]CH_3COO$ in MeCN.

The formation of the 1:1 complex comes with the quenching of the pyrene emission at 394 nm, and quenching is almost complete on addition of a 20-fold excess of CH_3COO^-. Moreover, a very moderate, poorly detectable emission band appears at 500 nm. Such an emission band is clearly distinguishable in the normalized spectrum shown in Figure 11b. Emission at 500 nm has to be ascribed to the excited tautomer $[L^2\cdots H{-}OOCCH_3]^-$*, which forms to some extent also in the less polar medium MeCN (whereas for L^1H it formed only in DMSO). It is suggested that $[L^2\cdots H{-}OOCCH_3]^-$* is stabilized with respect to $[L^1\cdots H{-}OOCCH_3]^-$* due to a more extended π-delocalization of the negative charge over the polyaromatic moiety. Thus, deactivation of the locally excited complex $[*L^2H\cdots X]^-$ takes place according the two parallel mechanisms: an eT process, as illustrated by route (a) in Figure 5 (predominant) and the conversion to the excited tautomer (route (c) in Figure 5).

The L^2H/F^- System: A Unique Optical Response. On UV−vis titration with $[Bu_4N]F$ of an MeCN solution of L^2H, the typical red shift of the absorption band was observed, as illustrated in Figure 11. Best fitting of titration data was obtained on assuming the formation of a 1:1 complex, according to the equilibrium $L^2H + F^- \leftrightarrows [L^2H\cdots F]^-$, with a log K = 4.45(1).

However, on addition of a large excess of fluoride (>100 equiv), the pale-yellow solution took an intense and bright-yellow color, while a new band developed at 450 nm, whose intensity reached a limiting value at ∼1000 equiv (see Figure 12).

Appearance of a new intense absorption band at longer wavelengths on addition of excess fluoride typically signals the deprotonation of one N−H fragment of the urea subunit, according to the equilibrium: $[L^2H\cdots F]^- + F^- \leftrightarrows [L^2]^- + HF_2^-$.

The occurrence of such a process has been confirmed by ^1H NMR studies in d^6-DMSO (see Figure S9). As a matter of fact, in the presence of excess fluoride, the signals of the urea's N−H protons disappear, and most of aromatic C−H signals are remarkably shifted upfield, except for C−H_α and C−H_β of the pyrenyl moiety, for which downfield shift was observed. Upfield shift of aromatic C−H is a signature of deprotonation of arylureas and has to be ascribed to an increase of electron density associated to the delocalization of the negative charge over the polyaromatic system.[7] On the other hand, the downfield shift of C−H_α and C−H_β protons may be attributed to the polarization effect exerted by the carbonyl oxygen atom, which has been made partially negative by urea deprotonation.

dx.doi.org/10.1021/ja4019786 | J. Am. Chem. Soc. 2013, 135, 6345−6355

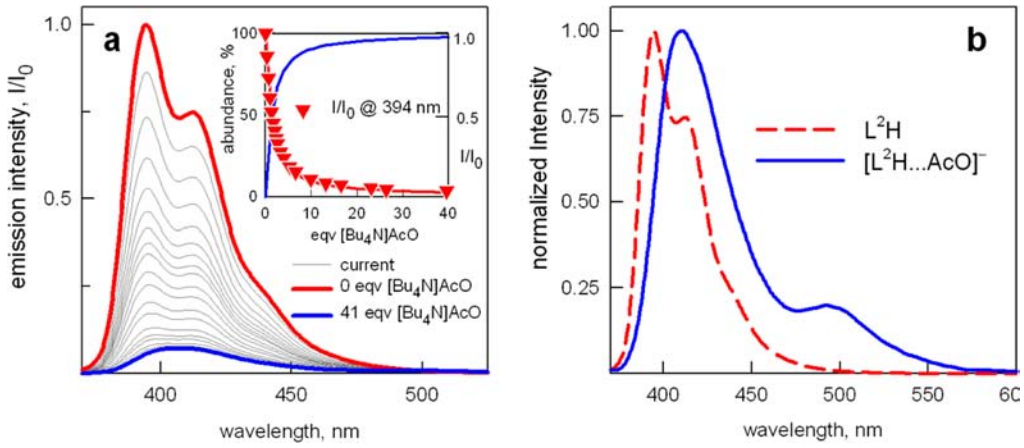

Figure 10. (a) Emission spectra taken upon titration of L^2H (0.01 mM) in MeCN with $[Bu_4N]CH_3COO$. Inset: lines are concentration profiles of the species at the equilibrium: L^2H (red) and $[L^2H\cdots CH_3COO]^-$ (blue), left vertical axis; and symbols are relative emission intensities at 394 nm, right vertical axis. T = 25 °C. (b) Normalized spectra of L^2H in the absence (red dashed line) and in the presence of an excess of $[Bu_4N]CH_3COO$ (blue solid line).

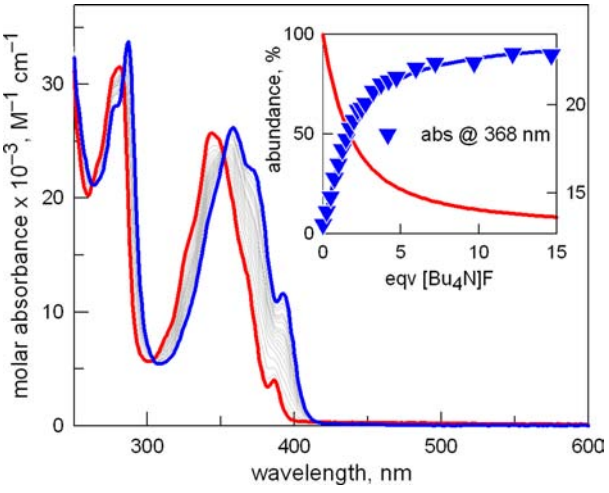

Figure 11. UV−vis spectra taken over the course of titration of receptor L^2H (0.03 mM) with $[Bu_4N]F$ in MeCN. Inset: lines are concentration profiles of the species at the equilibrium: L^2H (red line) and $[L^2H\cdots F]^-$ blue line, left vertical axis; and symbols are absorbance at 368 nm, right vertical axis.

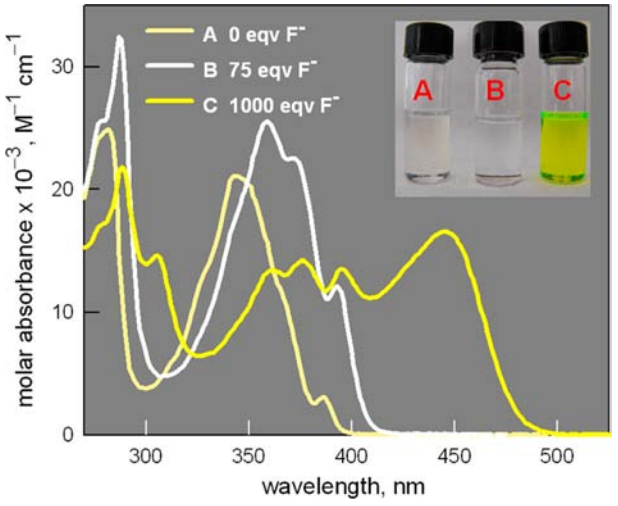

Figure 12. UV−vis spectra taken upon addition of $[Bu_4N]F$ to receptor L^2H (0.01 mM) in MeCN. Pale-yellow line (L^2H, vial A in the inset: ON^1); white line is spectrum taken after the addition of 75 equiv of $[Bu_4N]F$ (corresponding to $[L^2H\cdots F]^-$, vial B in the inset figure); bright-yellow line is spectrum taken after the addition of 1000 equiv of $[Bu_4N]F$ (corresponding to $[L_2]^-$, vial C in the inset).

Noticeably, allowing the solution of $[L^2]^-$ to stand exposed to air for 24 h, a reverse color change was observed, due to the acid−base reaction of $[L^2]^-$ with CO_2 and formation of the $[L^2H\cdots HCO_3]^-$ complex. This was substantiated by the recovery of N−H signals in the ^1H NMR spectrum. In particular, the obtained pattern is consistent with the formation of a complex of HCO_3^- (see Figure S9). CO_2 uptake in the presence of excess fluoride with formation of a crystalline hydrogencarbonate complex was first observed with the N−H containing receptor 4-amino-1,8-naphthalimide in DMSO,[20] a phenomenon which was later reported to occur in an MeCN solution of 1,3-bis-(4-nitro-phenyl)-urea.[8f]

The fluorimetric response of L^2H to fluoride is intriguing. A solution 0.01 mM in L^2H shows the typical pyrene emission with a maximum at $\lambda_{em\text{-}1}$ = 394 nm (blue fluorescence, ON^1 state, cyan line in Figure 13). Upon addition of $[Bu_4N]F$ over the 0−0.75 mM concentration interval, the emission is almost completely quenched, with the formation of the 1:1 complex (state OFF, white line in Figure 13).

On least-squares treatment of titration data over the 0 → 75 equiv interval of added F^- (see family of spectra in Figure S10), a log K_{fluo} = 4.52(1), was obtained for the 1:1 complexation equilibrium, a value comparable to that obtained by UV−vis titration (see Table 1). The drastic reduction of the fluorescence emission may be ascribed to two parallel mechanisms, as pictorially illustrated in Figure 14: (a) the occurrence of an eT process within the $[^*L^2H\cdots F]^-$ excited complex and (b) the conversion of $[^*L^2H\cdots F]^-$ to the poorly emissive excited tautomer $[L^2\cdots H{-}F]^{-*}$. Occurrence of route (b), at least to some extent, is indicated by weak, still detectable emission band centered at 500 nm. Then, upon further addition of fluoride (0.75 mM < $[Bu_4N]F$ < 10 mM), a yellow fluorescence turned on, while a new band appeared the emission spectrum ($\lambda_{em\text{-}2}$ = 500 nm, state ON^2, see Figure 13). UV−vis and ^1H NMR titration experiments have demonstrated that on a large excess addition of fluoride to L^2H, urea deprotonation takes place. Thus, the yellow fluorescence has to

dx.doi.org/10.1021/ja4019786 | J. Am. Chem. Soc. 2013, 135, 6345−6355

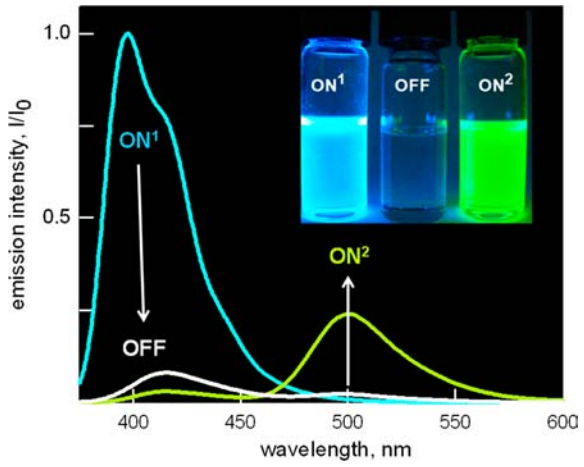

Figure 13. Emission spectra taken upon addition of $[Bu_4N]F$ to L^2H (0.01 mM) in MeCN. Cyan line is spectrum of the free receptor (L^2H, ON^1); white line is spectrum of L^2H taken upon addition of 75 equiv of $[Bu_4N]F$ (corresponding to $[L^2H\cdots F]^-$, OFF); and yellow line is spectrum taken after the addition of 1000 equiv of $[Bu_4N]F$ (corresponding to $[L^2]^-$, ON^2). Inset: pictures of samples taken in the dark on UV illumination.

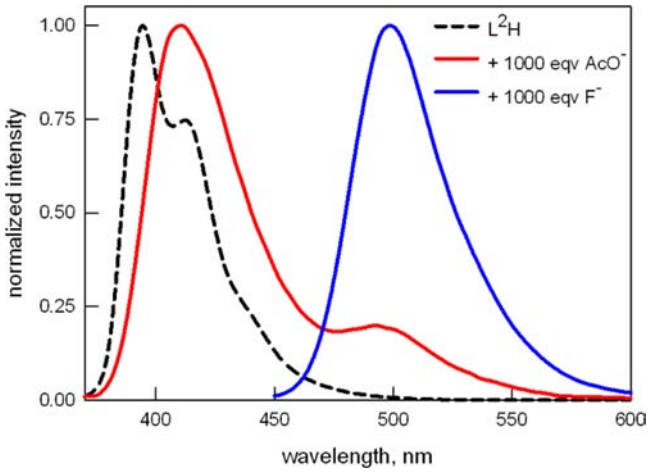

Figure 15. Normalized emission spectra of L^2H (0.01 mM, black dashed line, λ_{exc} = 348 nm), in the presence of excess $[Bu_4N]$-CH_3COO (10 mM, red solid line) and $[Bu_4N]F$ (10 mM, blue solid line) in MeCN. Corresponding excitation spectra are shown in Figure S11.

be ascribed to a charge-transfer emission by the deprotonated receptor $[L^2]^-$. The nature of the ON^1-OFF−ON^2 behavior is pictorially illustrated in Figure 14.

Figure 15 shows the normalized spectrum of MeCN solutions of L^2H and L^2H + 1000 equiv of $[Bu_4N]F$, which contains the deprotonated receptor $[L^2]^-$. The normalized spectrum obtained in the presence of the same excess of $[Bu_4N]CH_3COO$ is also shown for comparative purposes.

It is worth noting that the low-energy emission of the $[L^2H\cdots CH_3COO]^-$ complex, due to the tautomeric excited state $[L^2\cdots H{-}OOCCH_3]^-*$, and the emission of $[L^2]^-*$ fall at the same wavelength. This seems quite reasonable, because the emitting fluorophore is the same, i.e., the excited deprotonated receptor, whether inside the H-bond complex or as an uncomplexed anion.

The L^2H/F^- system is a member of the rich family of three-state molecular photoionic switches, i.e., molecules or ensembles of molecules capable to release a fluorescent signal (the output) as a consequence of the change of the concentration of a given ion (the input). The first example, due to de Silva, consisted in an anthracenyl moiety covalently linked to a tertiary amine group and to a pyridine fragment.[21] On addition of H^+, the fluorescent output varied according to an OFF−ON−OFF mode. A number of OFF−ON−OFF fluorescence switches driven by a pH change have been described in the following years.[22] Some OFF−ON−OFF luminescence switches operated by mixed ionic inputs, (Zn^{2+}, K^+)[23] and (Cu^{2+}, F^-),[24] have been recently reported. The first ON−OFF−ON fluorescence switch, driven by a protonic input, dates back to 2002,[25] followed by more recent systems operating in an analogous way.[26] In all these systems the same fluorescent emission is switched off/on on increasing/

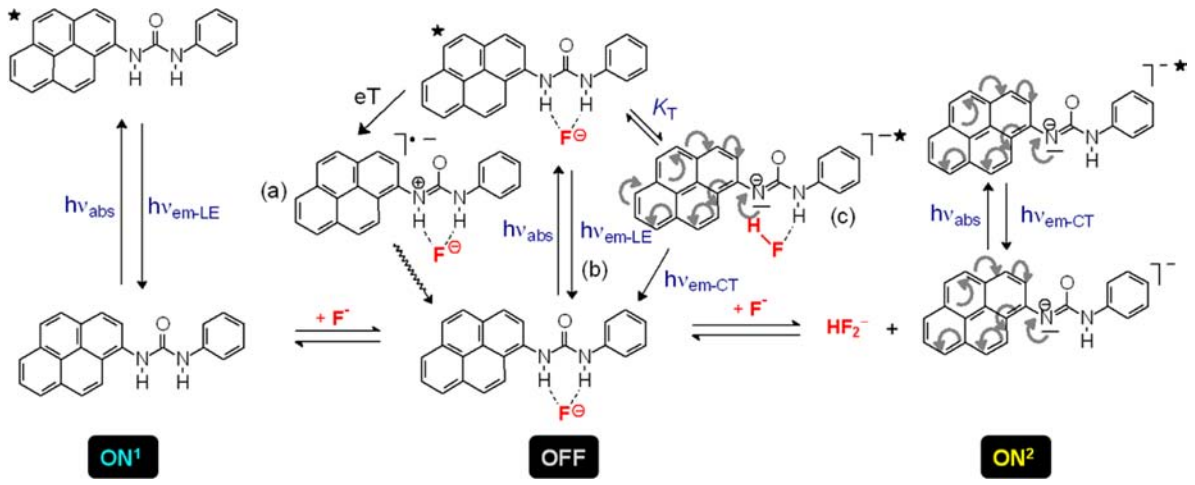

Figure 14. A qualitative sketch of the emissive behavior of L^2H in MeCN on addition of varying amounts of $[Bu_4N]F$. On addition of fluoride up to 75 equiv, the H-bond complex $[L^2H\cdots F]^-$ forms, while pyrene fluorescence is drastically reduced, due to an intracomplex eT process (route a) and/or to the formation of the poorly emissive excited tautomer $[L^2\cdots H{-}F]^-*$. On further addition of $[Bu_4N]F$, a yellow fluorescence is switched on, thanks to the distinctive emitting behavior of $[L^2]^-$, formed on deprotonation of one urea's N−H fragment. The π-delocalization scheme over the pyrenyl subunit in the excited tautomer $[L^2\cdots H{-}F]^-*$ and in both ground state and excited deprotonated receptor $[L^2]^-$ is purely indicative.

dx.doi.org/10.1021/ja4019786 | J. Am. Chem. Soc. 2013, 135, 6345−6355

decreasing pH (ON^1−OFF−ON^1 output). An ON^1−OFF−ON^1 photoswitch driven by a mixed output (Cu^{2+}, Ag^+) has been recently described.[27] The ON^1−OFF−ON^2 output is more rare: besides the two systems of the type receptor/F^-, previously reported,[11] and described here, it was observed with a chelating agent containing the methoxy-quinoline subunit and was driven by a change of the concentration of Ag^+.[28]

CONCLUSION

L^1H and L^2H are simple molecules and anion sensors of poorly sophisticated design. Nevertheless, their optical response is multifaceted, in some cases surprising, and can teach some useful lessons to people interested in the design of urea-based derivatives for recognition and sensing of anions. In particular, significantly different optical responses have been observed depending on the nature of the chromophore/fluorophore covalently linked to the urea subunit (whether 2-anthracenyl or 1-pyrenyl) and on the properties of the envisaged anion. Poorly basic anions (Cl^-, Br^-) form with L^1H and L^2H 1:1 H-bond complexes, $[L{-}H{\cdots}X]^-$, which are stable in both ground and excited states, and their recognition is signaled by the red shift of both absorption and emission bands. Basic anions (e.g., carboxylates) form with L^1H more stable complexes than halides, and in an MeCN solution, an intracomplex electron transfer takes place, which quenches the blue fluorescence. However, for L^1H in DMSO and for L^2H in both MeCN and DMSO, an intracomplex proton transfer takes place in the locally excited complex $[{*}L{-}H{\cdots}X]^-$ to form the excited tautomer $[L{\cdots}H{-}X]^{-}{*}$, which gives rise to a weak emission at higher wavelengths, of charge-transfer nature. Fluoride is special because it forms with L^1H a stable $[L{-}H{\cdots}F]^-$ complex, which in the excited state undergoes intracomplex proton transfer, to give the weakly emissive excited tautomer $[L{\cdots}H{-}F]^{-}{*}$. On the other hand, with receptor L^2H, excess fluoride promotes deprotonation of the ground-state complex, according to the equilibrium $[L^2H{\cdots}F]^- + F^- \leftrightarrows [L^2]^- + HF_2^-$. The deprotonated receptor $[L^2]^-$ is distinctly emissive (yellow fluorescence), a circumstance which generates the fluorimetric response ON^1−OFF−ON^2 of receptor L^2H with respect to F^-.

These optical features are not necessarily restricted to urea derivatives and could be reasonably observed in other neutral receptors containing N−H fragments (amides, thioureas, etc.), which may open new perspectives in the design of fluorescent sensors for anions. Research in this area is currently underway in this laboratory.

ASSOCIATED CONTENT

Supporting Information

Synthesis and characterization of L^1H and L^2H; details on crystallographic studies (ORTEP views, tables with bond distances and angles of H-bonding interactions); spectra taken over the course of UV−vis, emission and ^1H NMR titration experiments; excitation and emission spectra in BuCN at 77 K. This material is available free of charge via the Internet at http://pubs.acs.org.

AUTHOR INFORMATION

Corresponding Author

valeria.amendola@unipv.it; luigi.fabbrizzi@unipv.it

Notes

The authors declare no competing financial interest.

ACKNOWLEDGMENTS

This research was supported by the Italian Ministry of University and Research (project PRIN: InfoChem).

REFERENCES

(1) *Anion Coordination Chemistry*; Bowman-James, K., Bianchi, A., García-España, E., Eds; Wiley-VCH: Weinheim, 2011.
(2) (a) Santos-Figueroa, L. E.; Moragues, M. E.; Climent, E.; Agostini, A.; Martínez-Máñez, R.; Sancenón, F. *Chem. Soc. Rev.* **2013**, *42*, 3489−3613. (b) Wenzel, M.; Hiscock, J. R.; Gale, P. A. *Chem. Soc. Rev.* **2012**, *41*, 480−520.
(3) Hossain, M. A.; Begum, R. A.; Day, V. W.; Bowman-James, K. Amide and urea-based receptors. *Supramolecular Chemistry: From Molecules to Nanomaterials*; Wiley: Hoboken, NJ, 2012; Vol. *3*, pp 1153−1178.
(4) Li, A.-F.; Wang, J.-H.; Wang, F.; Jiang, Y.-B. *Chem. Soc. Rev.* **2010**, *39*, 3729−3745.
(5) Amendola, V.; Fabbrizzi, L.; Mosca, L. *Chem. Soc. Rev.* **2010**, *39*, 3889−3915.
(6) Cametti, M.; Rissanen, K. *Chem. Soc. Rev.* **2013**, *42*, 2016−2038.
(7) Amendola, V.; Esteban-Gómez, D.; Fabbrizzi, L.; Licchelli, M. *Acc. Chem. Res.* **2006**, *39*, 343−353.
(8) (a) Bergamaschi, G.; Boiocchi, M.; Monzani, E.; Amendola, V. *Org. Biomol. Chem.* **2011**, *9*, 8276−8283. (b) Amendola, V.; Fabbrizzi, L.; Mosca, L.; Schmidtchen, F. P. *Chem.—Eur. J.* **2011**, *17*, 5972−5981. (c) Esteban-Gómez, D.; Fabbrizzi, L.; Licchelli, M.; Monzani, E. *Org. Biomol. Chem.* **2005**, *3*, 1495−1500. (d) Esteban-Gómez, D.; Fabbrizzi, L.; Licchelli, M. *J. Org. Chem.* **2005**, *70*, 5717−5720. (e) Boiocchi, M.; Del Boca, L.; Esteban-Gómez, D.; Fabbrizzi, L.; Licchelli, M.; Monzani, E. *Chem.—Eur. J.* **2005**, *11*, 3097−3104. (f) Boiocchi, M.; Del Boca, L.; Esteban-Gómez, D.; Fabbrizzi, L.; Licchelli, M.; Monzani, E. *J. Am. Chem. Soc.* **2004**, *126*, 16507−16514.
(9) (a) Jiménez, D.; Martínez-Máñez, R.; Sancenón, F.; Soto, J. *Tetrahedron Lett.* **2002**, *43*, 2823−2825. (b) Jose, D. A.; Kumar, D. K.; Ganguly, B.; Das, A. *Org. Lett.* **2004**, *6*, 3445−3448. (c) Gunnlaugsson, T.; Davis, A. P.; O'Brien, J. E.; Glynn, M. *Org. Biomol. Chem.* **2005**, *3*, 48−56. (d) Rena, J.; Zhaoa, X.-L.; Qiao-Chun Wanga, Q.-C.; Kub, C.-F.; Qua, D.-H.; Chang, C.-P.; Tian, H. *Dyes Pigm.* **2005**, *64*, 193−200. (e) Mikláš, R.; Kasák, P.; Devínsky, F.; Putala, M. *Chemical Papers* **2009**, *63*, 709−715. (f) Ghosh, A.; Verma, S.; Ganguly, B.; Ghosh, H. N.; Das, A. *Eur. J. Inorg. Chem.* **2009**, 2496−2507. (g) Bhardwaj, V. K.; Sharma, S.; Singh, N.; Hundal, M. S.; Hundal, G. *Supramol. Chem.* **2011**, *23*, 790−800. (h) Duke, R. M.; Gunnlaugsson, T. *Tetrahedron Lett.* **2011**, *52*, 1503−1505. (i) Zhou, Y.-P.; Zhang, M.; Li, Y.-H.; Guan, Q.-R.; Wang, F.; Lin, Z.-J.; Lam, C.-K.; Feng, X.-L.; Chao, H.-Y. *Inorg. Chem.* **2012**, *51*, 5099−5109. (j) Kim, D. W.; J Kim, J.; Hwang, J.; Park, JJ. K.; Kim, J. S. *Bull. Korean Chem. Soc.* **2012**, *33*, 1159−1163. (k) Dong, Z.-Y.; Gao, G.-H. *Chin. Sci. Bull.* **2012**, *57*, 1266−1274.
(10) (a) Ikedu, S.; Nishimura, Y.; Tatsuo Arai, T. *J. Phys. Chem. A* **2011**, *115*, 8227−8233. (b) Ohshiro, I.; Ikegami, M.; Shinohara, Y.; Nishimura, Y.; Arai, T. *Bull. Chem. Soc. Jpn.* **2007**, *80*, 747−751.
(11) Luxami, V.; Kumar, S. *Tetrahedron Lett.* **2007**, *48*, 3083−3087.
(12) (a) Gans, P.; Sabatini, A.; Vacca, A. *Talanta* **1996**, *43*, 1739−1753. (b) *Hyperquad2008: Potentiometric data*; http://www.hyperquad.co.uk/index.htm, accessed on 20 February 20, 2013
(13) *SAINT Software Reference Manual*, version 6; Bruker AXS, Inc., Madison, Wisconsin, 2003.
(14) Sheldrick, G. M. *SADABS Siemens Area Detector Absorption Correction Program*; University of Göttingen: Göttingen, Germany, 1996.
(15) Altomare, A.; Burla, M. C.; Camalli, M.; Cascarano, G. L.; Giacovazzo, C.; Guagliardi, A.; Moliterni, A. G. G.; Polidori, G.; Spagna, R. *J. Appl. Crystallogr.* **1999**, *32*, 115−119.
(16) Sheldrick, G. M. *Acta Crystallogr.* **2008**, *A64*, 112−122.
(17) Steiner, T. *Angew. Chem., Int. Ed.* **2002**, *41*, 48−76.
(18) (a) Kerr, C. E.; Mitchell, C. D.; Headrick, J.; Eaton, B. E.; Netzel, T. L. *J. Phys. Chem. B* **2000**, *104*, 1637−1650. (b) Pereira, R. V.; Gehlen, M. H. *Chem. Phys. Lett.* **2006**, *426*, 311−317.

(19) (a) Brooks, S. J.; Edwards, P. R.; Gale, P. A.; Light, M. E. *New J. Chem.* **2006**, *30*, 65−70. (b) Formica, M.; Fusi, V.; Macedi, E.; Paoli, P.; Piersanti, G.; Rossi, P.; Zappia, G.; Orlando, P. *New J. Chem.* **2008**, *32*, 1204−1214.
(20) Gunnlaugsson, T.; Kruger, P. E.; Jensen, P.; Frederick, M.; Pfeffer, F. M.; M. Hussey, G. M. *Tetrahedron Lett.* **2003**, *44*, 8909−8913.
(21) de Silva, A. P.; Gunaratne, H. Q. N.; McCoy, C. P. *Chem. Commun.* **1996**, 2399−2400.
(22) (a) Fabbrizzi, L.; Gatti, F.; Pallavicini, P.; Parodi, L. *New J. Chem.* **1998**, 1403−1407. (b) de Silva, S. A.; Amorelli, B.; Isidor, D. C.; Loo, K. C.; Crooker, K. E.; Pena, Y. E. *Chem. Commun.* **2002**, 1360−1361. (c) Callan, J. F.; de Silva, A. P.; McClenaghan, N. D. *Chem. Commun.* **2004**, 2048−2049. (d) Brown, G. J.; de Silva, A. P; James, M. R.; McKinney, B. O. F.; Pears, D. A.; Weir, S. M. *Tetrahedron* **2008**, *64*, 8301−8306. (e) Aucejo, R.; Alarcón, J.; García-España, E.; Llinares, J. M.; Marchin, K. L.; Soriano, C.; Lodeiro, C.; Bernardo, M. A.; Pina, F.; Seixas de Melo, J. *Eur. J. Inorg. Chem.* **2005**, 4301−4308. (f) de Silva, S. A.; Loo, K. C.; Amorelli, B.; Pathirana, S. L.; Nyakirang'ani, M.; Dharmasena, M.; Demarais, S.; Dorcley, B.; Pullay, P.; Salih, Y. A. *J. Mater. Chem.* **2005**, *15*, 2791−2795. (g) Han, M.-J.; Gao, L.-H.; Lu, Y. Y.; Wang, K.-Z. *J. Phys. Chem. B* **2006**, *110*, 2364−2371. (h) Pais, V. P.; Remón, P.; Collado, D.; Andréasson, J.; Pérez-Inestrosa, E. P.; Pischel, U. *Org. Lett.* **2011**, *13*, 5572−5575. (i) Sadhu, K. K.; Mizukami, S.; Yoshimura, A.; Kikuchi, K. *Org. Biomol. Chem.* **2013**, *11*, 563−568.
(23) Li, Y.-P; Yang, H.-R.; Zhao, Q.; Song, W.-C.; Han, J.; Bu, X.-H. *Inorg. Chem.* **2012**, *51*, 9642−9648.
(24) Peng, Y.; Dong, Y.-M.; Dong, M.; Wang, Y.-W. *J. Org. Chem.* **2012**, *77*, 9072−9080.
(25) Amendola, V.; Fabbrizzi, L.; Mangano, C.; Miller, H.; Pallavicini, P.; Perotti, P.; Taglietti, A. *Angew. Chem., Int. Ed.* **2002**, *41*, 2553−2556.
(26) (a) Pallavicini, P.; Amendola, V.; Massera, C.; Mundum, E.; Taglietti, A. *Chem. Commun.* **2002**, 2452−2453. (b) Yao, J.-L.; Gao, X.; Sun, W.; Fan, X.-Z.; Shi, S.; Yao, T.-M. *Inorg. Chem.* **2012**, *51*, 12591−12593. (c) Zhao, X.-L.; Ma, Y.-Z.; Wang, K.-Z. *J. Inorg. Biochem.* **2012**, *113*, 66−76.
(27) Pandey, R.; Kumar, P.; Singh, A. K.; Shahid, M.; Li, P.; Singh, S. K.; Xu, Q.; Misra, A.; Pandey, D. S. *Inorg. Chem.* **2011**, *50*, 3189−3197.
(28) Singh, P.; Kumar, S. *Tetrahedron Lett.* **2006**, *47*, 109−112.